Electronic Supplementary Material (ESI) for Chemical Communications.

Supporting Information

Oxygen-reduction catalysis of N-doped carbons prepared by heat treatment of polyaniline at over 1100 ºC

Javier Quílez-Bermejo, Emilia Morallón, Diego Cazorla-Amorós

Experimental

1. Materials.

Aniline was purchased from Sigma Aldrich and distilled by refluxing under reduced pressure prior its use in order to remove the impurities. Ammonium persulfate ($(NH_4)_2(S_2O_8)$), ammonium hydroxide (NH_4OH), potassium hydroxide (KOH) and 20wt% Pt/Vulcan were purchased from Sigma Aldrich. Perchloric acid (60%, $HClO_4$) was purchased from VWR-Chemicals Prolabo. All the solutions were prepared using ultrapure water (18MΩ cm from an Elga Labwater Purelab system). The gases N_2 (99.999%), O_2 (99.995%), H_2 (99.999%) and synthetic air were provided by Air Liquide and were used without any further purification or treatment.

2. PANI preparation.

Polyaniline was prepared by chemical polymerization from a solution of 1M HCl containing 0.67M of aniline and ammonium persulfate in a stoichiometric ratio. The mixture was kept under stirring (500rpm) for 3 h at 0ºC. In order to obtain the dedoped-polyaniline, polyaniline was treated with 1M NH_4OH for 24h. The synthesized PANI was washed several times with distilled water and dried at 80ºC overnight.

3. Heat treatment.

The samples of PANI (150 mg) were heat treated in a tubular furnace at different temperatures between 600 and 1200ºC for 1h using a heating rate of 5ºC min^{-1} in a nitrogen-atmosphere. The final carbon material is named as PANI_X, being X the carbonization temperature used during the heat treatment. All PANI-derived carbon materials are obtained as a powder (from the TEM image in Figure S16, it is possible to observe that the particles are below 1 µm and are formed by aggregation of individual nanosized particles of around 20-200 nm). The furnace was purged for 1h before the heat treatment in the corresponding atmosphere, the flow rate was maintained at 100ml min^{-1} during the treatment. The same treatmet was carried out in presence of argon-atmosphere in order to confirm the inert properties of the nitrogen-atmosphere at the experimental conditions used. The resulting material is named as PANI_Ar_X, where X is the temperature used during the heat treatment.

4. Characterization.

The study of the electrocatalytic activity towards ORR was performed in an Autolab PGSTAT302 (Metrohm, Netherlands) potentiostat. A rotating ring-disk electrode (RRDE, Pine Research Instruments, USA) equipped with a glassy carbon disk (5.61 mm diameter) and an attached platinum ring was used as the working electrode. A platinum wire was used as the counter electrode and a reversible hydrogen electrode immersed in the working electrolyte as the reference electrode. The amount of catalyst on the disk electrode was optimized in order to reach the highest limiting current, being 120 µg the optimum value. Therefore, the glassy carbon disk was modified with the samples using 120 µl of a 1 $mg \cdot ml^{-1}$ dispersion of each carbon material (20% isopropanol, 0.02% Nafion ®), obtaining a catalyst loading of 0.48 mg cm^{-2}. The electrocatalytic activity towards ORR was studied by linear sweep voltammetry (LSV) in O_2 saturated 0.1 M KOH between 0.0 and 1.0 V (vs RHE) at different rotation rates, from 400 to 2025 rpm and at a scan rate of 5 mV s^{-1}. The potential of the ring was held constant at 1.5 V (vs.

RHE) during all measurements. The H_2O_2 yield and the number of electrons were calculated from the hydrogen peroxide oxidation in the Pt ring electrode as follows:

$$H_2O_2\ (\%) = 200 \times \frac{I_R/N}{\left(I_R/N\right) + I_D}$$

$$n = \frac{4I_D}{I_D + I_R/N}$$

where I_R and I_D are the current measured at the ring and the disk, respectively, and N is the collection efficiency of the ring, which was experimentally determined to be 0.37. The number of electrons and H_2O_2 generation was discussed by RRDE and not by Koutecky-Levich theory in order to reflect more faithfully the results obtained. Nevertheless, the number of electrons calculated by KL are included in the comparison with the bibliography in Table S2. Moreover, a rotating disk electrode (RDE, Pine Research Instruments, USA) equipped with a glassy carbon disk (5mm diameter) and graphite as a counter electrode was used in order to discard the possibility of Pt contamination from the counter electrode and platinum ring.

Thermogravimetric analysis has been performed using a thermobalance (SDT 2960 Instrument, TA). Heat treatment in air conditions (100 mL·min^{-1}) of carbon materials was characterized in air at 900 ^{o}C (heating rate of 10 ^{o}C·min^{-1}).

In order to study the stability performance and methanol poisoning test, chronoamperometric experiments were performed. The stability experiments were performed in 0.1 M KOH at a potential of 0.65 V and 1600rpm for 2 hours. In order to study the stability of the catalysts in presence of methanol, after the 2 hours of the stability test, methanol was added into the electrolyte until achieving 1M methanol.

The textural properties of the materials were evaluated by N_2 adsorption isotherms at -196ºC in an automatic adsorption system (Autosorb-6, Quantachrome). Prior to the measurements, the samples were degassed at 250ºC for 4h. Apparent surface areas have been determined by BET method (S_{BET}). Figure S7 includes the N_2 isotherms for three representative materials and the BET surface areas for all the materials prepared. The results show an increase in surface area with heat treatment temperature and that it reaches the highest values for heat treatment temperatures above 1000ºC. The development of porosity by carbonization of polymers is very much dependent on the physical and chemical properties of the precursor. In all the cases, the porosity goes through a maximum with increasing the heat treatment temperature but the values of porosity are dependent on the precursor. For example, in the case of infusible polymers like PVDC, surface areas as high as 1200 m^2/g are obtained at heat treatment temperatures of 1300 ºC, but in the case of fusible polymers like PFA, the maximum of surface area (around 450 m^2/g) is obtained at 750ºC (see reference S1).

PANI is an example of conjugated polymer that can be directly carbonized with good yields due to the strong intra and inter Pi-Pi interactions (see reference S2). And porous nanostructured carbons can be directly obtained through direct carbonization, that is, using template free strategies (see reference S2). In addition, very different porosities are obtained depending on the preparation conditions and even using the same template (see reference S2).

The samples were characterized by Transmission Electron Microscopy (TEM) coupled to EDX with a JEOL JEM-2010 microscope operating at 200kV with a spatial resolution of 0.24 nm.

The electrical conductivity of all samples was evaluated using electrochemical impedance spectroscopy (EIS) in an Autolab PGSTAT302. Impedance spectra were measured at 0.5 V vs. RHE in the frequency range of 10mHz to 100kHz with an amplitude for the voltage signal of 10 mV in 0.1M KOH solution.

Raman spectra were collected with a Jasco NRS-5100 spectrometer. A 3.9 mW He-Ne laser at 633 nm was used. The spectra were acquired for 120 s. The detector was a Peltier cooled charge-coupled device (CCD) (1024 x 255 pixels). Calibration of the spectrometer was performed with a Si slice (521 ± 2 cm^{-1}).

The surface composition and oxidation states of the elements of the prepared materials were studied using XPS in a VG-Microtech Multilab 3000 spectrometer with an Al Kα radiation source (1253.6 eV). The deconvolution of the N1s XPS spectra was done by least squares fitting using Gaussian-Lorentzian curves, while a Shirley line was used for the background determination.

The determination of the electronic density distribution was performed with Gaussian 09 using density functional theory (DFT) with b3lyp/6-31 g(d) level of approximation.

Figures and Tables

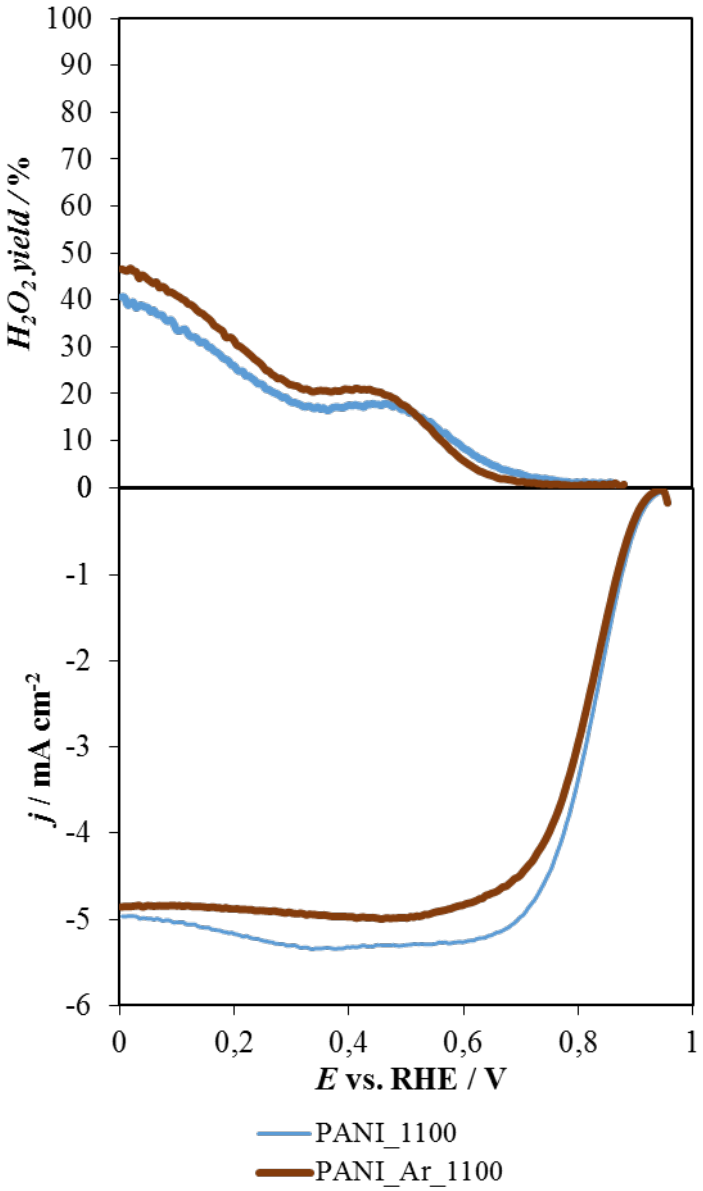

Figure S1: (a) H_2O_2 yield and (b) Linear sweep voltammetry curves of PANI_1100 and PANI_Ar_1100 in O_2-saturated 0.1 M KOH at 5mV s^{-1} and 1600rpm

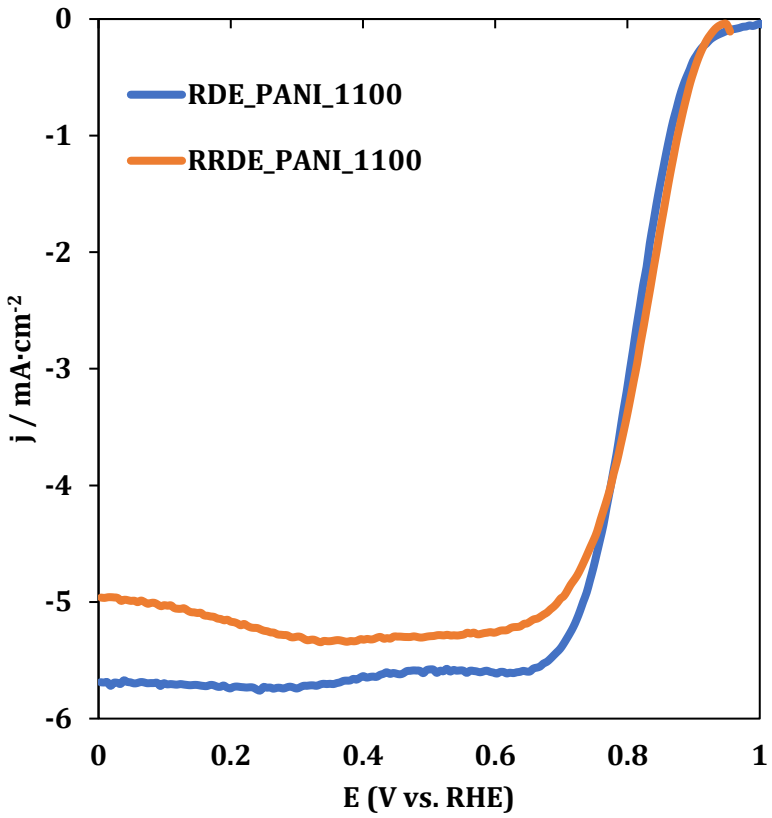

Figure S2: RDE study of PANI_1100 in O_2-saturated 0.1 M KOH at 5mV $\cdot s^{-1}$ at 1600rpm . RRDE measurement of the same sample was added for comparison purposes.

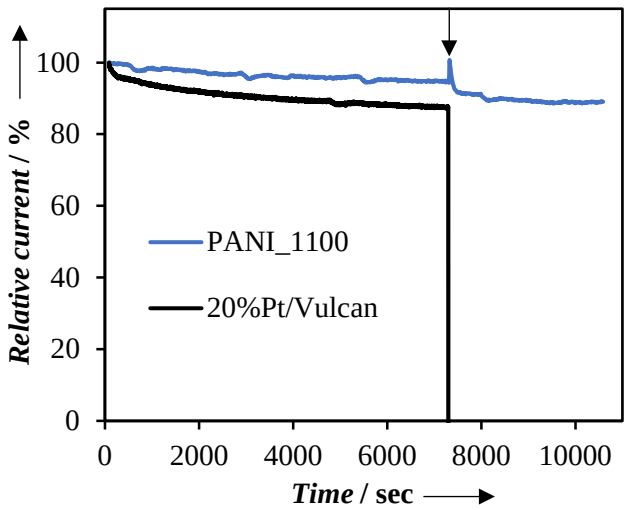

Figure S3: Current versus time for PANI_1100 and 20%Pt/Vulcan at 0.65V vs RHE in O_2-saturated 0.1M KOH solution at 1600rpm and 25ºC.

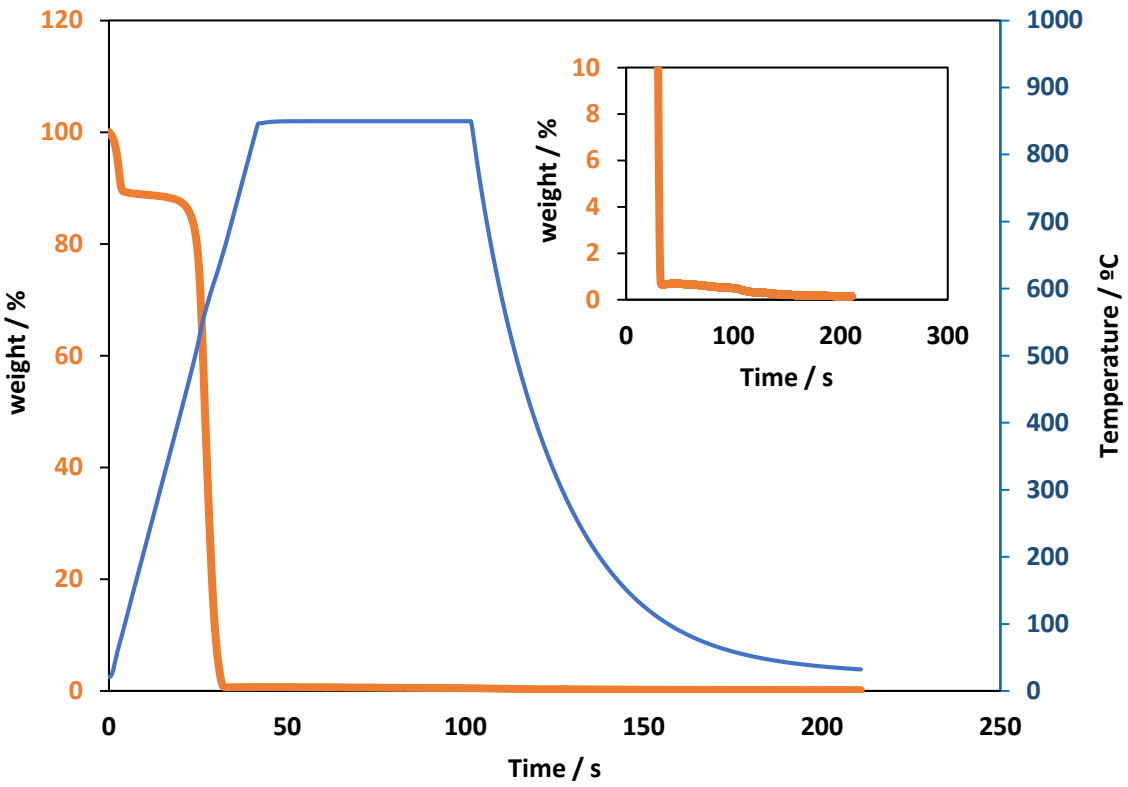

Figure S4: TG analysis profiles of PANI_1100 in air at 10ºC/min until 900 ºC in air atmosphere.

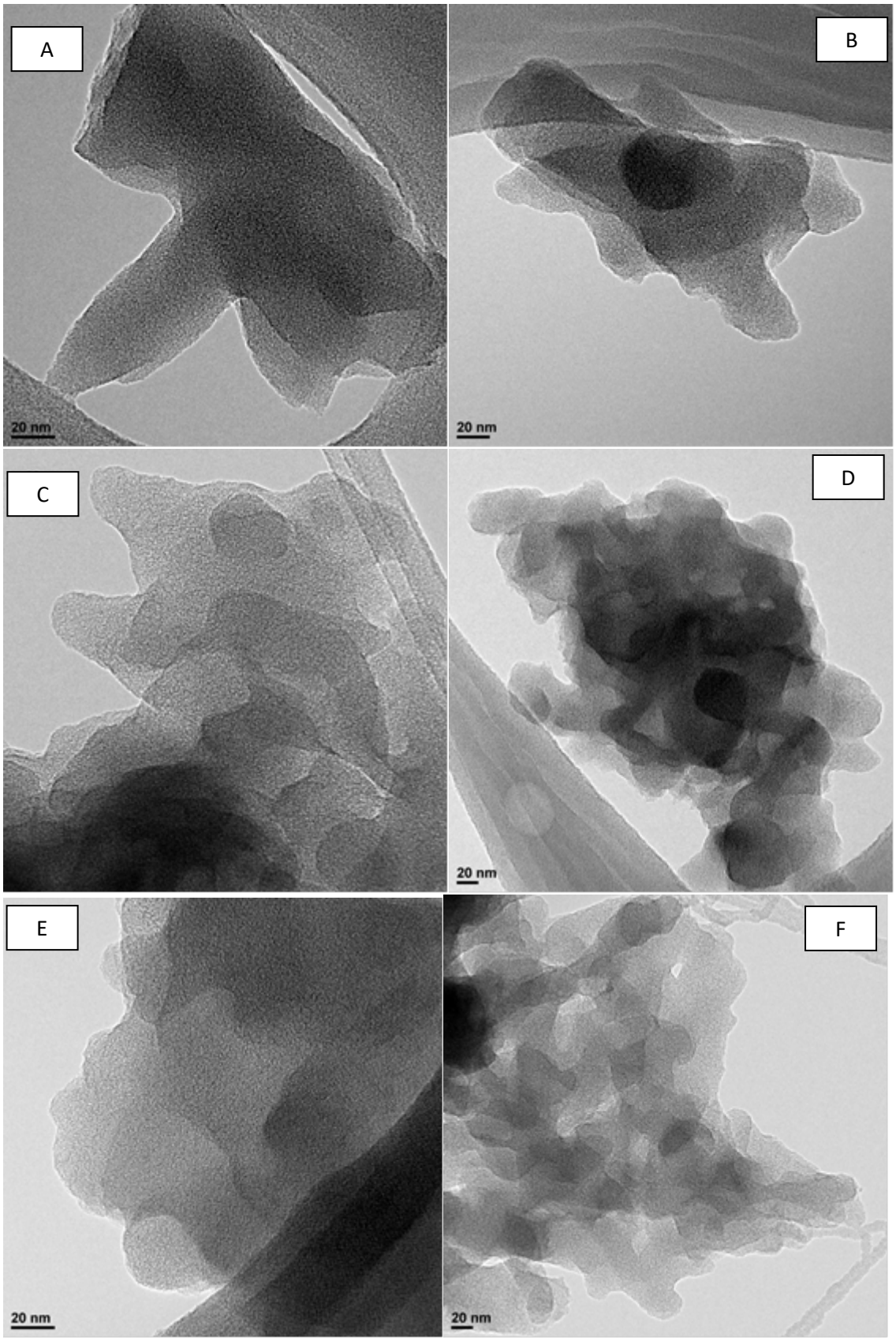

Figure S5: TEM images of (A) PANI_600, (B) PANI_800, (C) PANI_900, (D) PANI_1000, (E) PANI_1100 and (F) PANI_1200

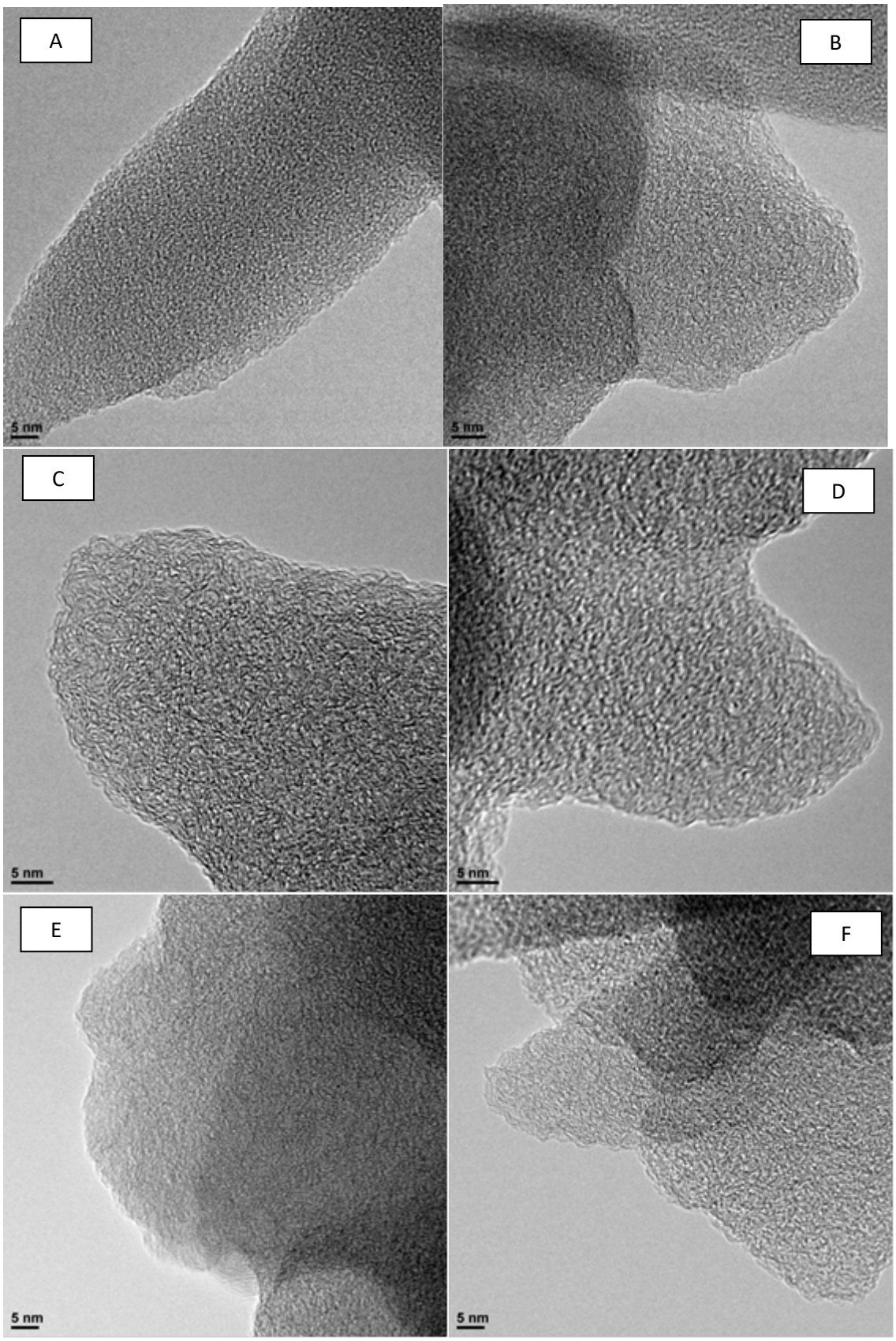

Figure S6: TEM images of (A) PANI_600, (B) PANI_800, (C) PANI_900, (D) PANI_1000, (E) PANI_1100 and (F) PANI_1200

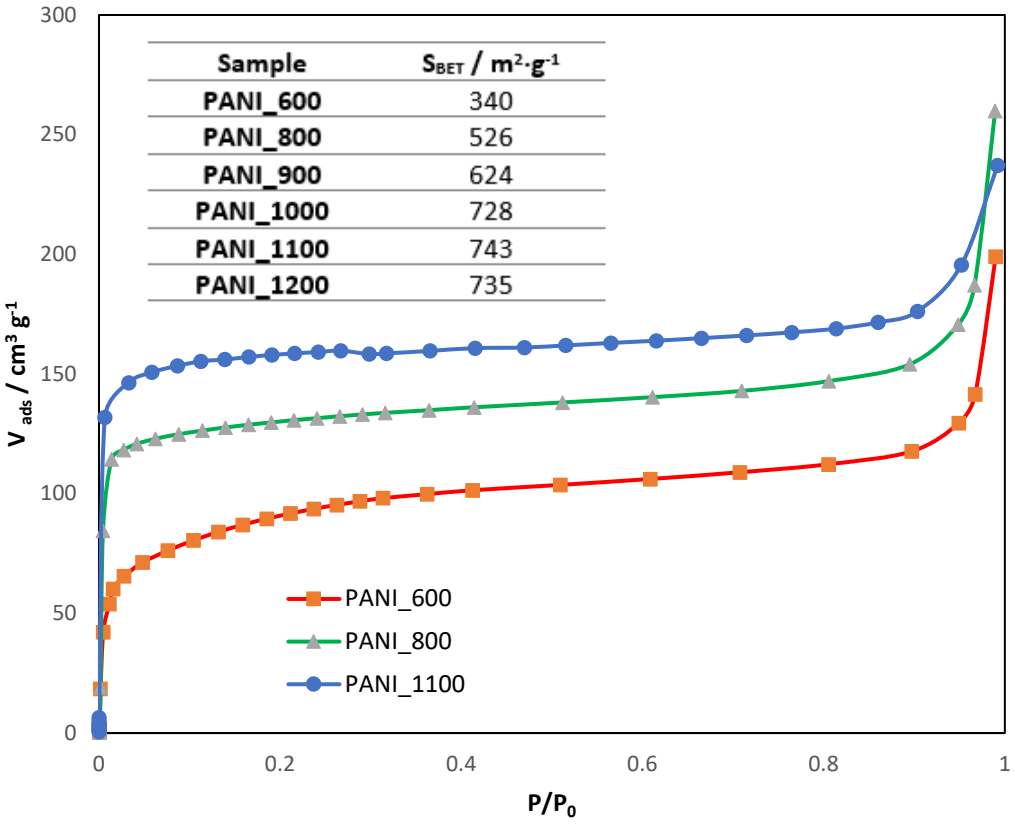

Figure S7: N_2 adsorption isotherms at -196 ^oC of the PANI-derived carbon materials prepared at 600, 800 and 1100 ^oC and surface area data for all the materials prepared.

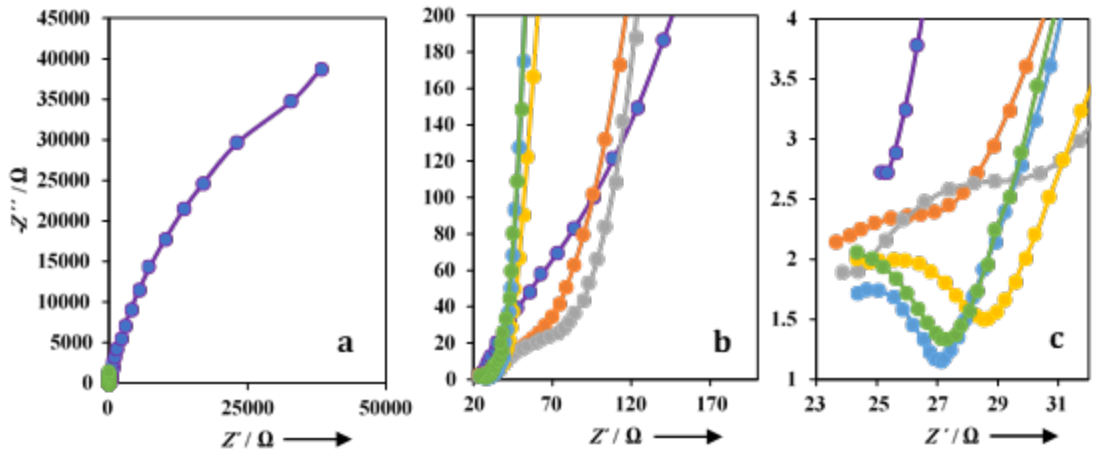

Figure S8: Nyquist plots corresponding to carbon materials obtained by heat treatment in N_2 atmosphere at 600ºC (violet line), 800ºC (grey line), 900ºC (red line), 1000ºC (yellow line), 1100 (blue line) and 1200ºC (green line) in 0.1 M KOH solution.

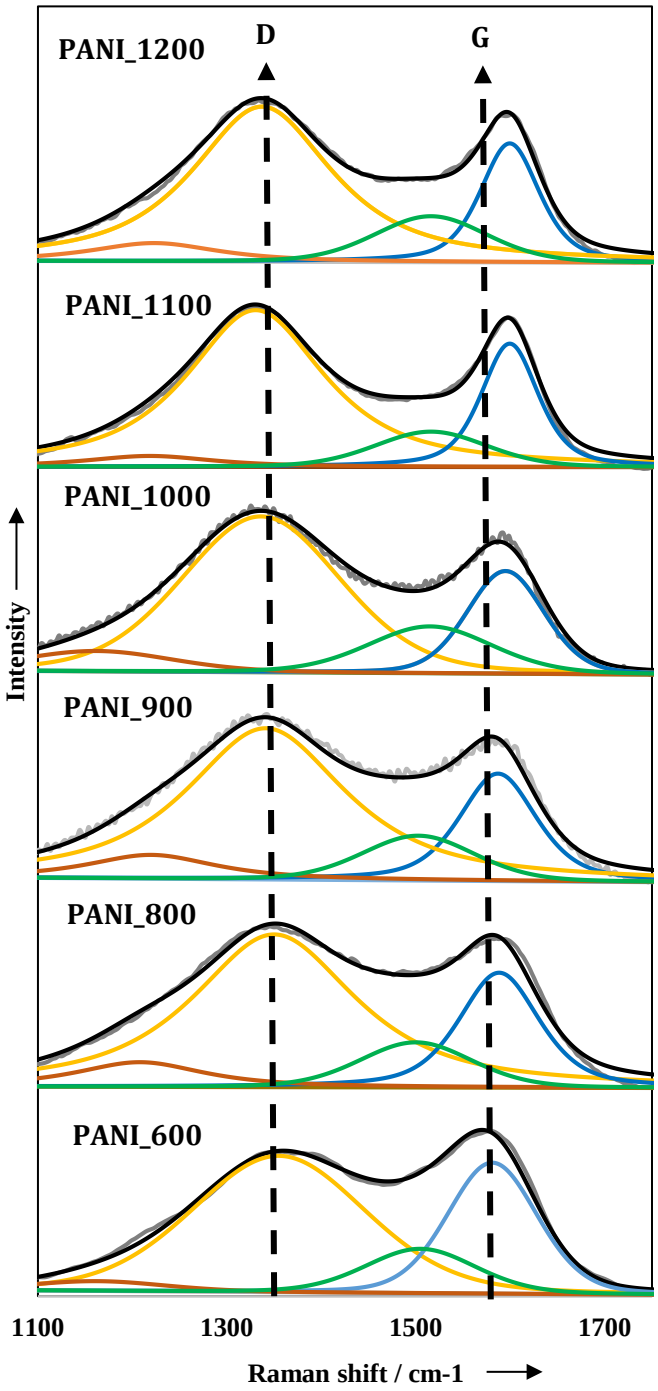

Figure S9: Raman spectra of all materials.

Table S1: Yield of the heat treatment (weight %), percentage of nitrogen and carbon contents (atomic %) and percentage of each nitrogen functional group for all materials.

SAMPLE	% YIELD	N CONTENT / %	C CONTENT / %	PYRIDINE N / %	PYRROL/PYRIDONE N / %	QUATERNARY N / %	OXIDIZED N / %	AMINES / %
PANI_600	61	7.7	86.9	29	49	-	-	22
PANI_800	53	7.0	90.2	40	35	25	-	-
PANI_900	49	4.3	91.0	35	34	26	5	-
PANI_1000	39	3.0	91.5	31	35	28	6	-
PANI_1100	32	1.8	93.4	24	34	32	10	-
PANI_1200	29	1.0	96.5	18	35	33	14	-

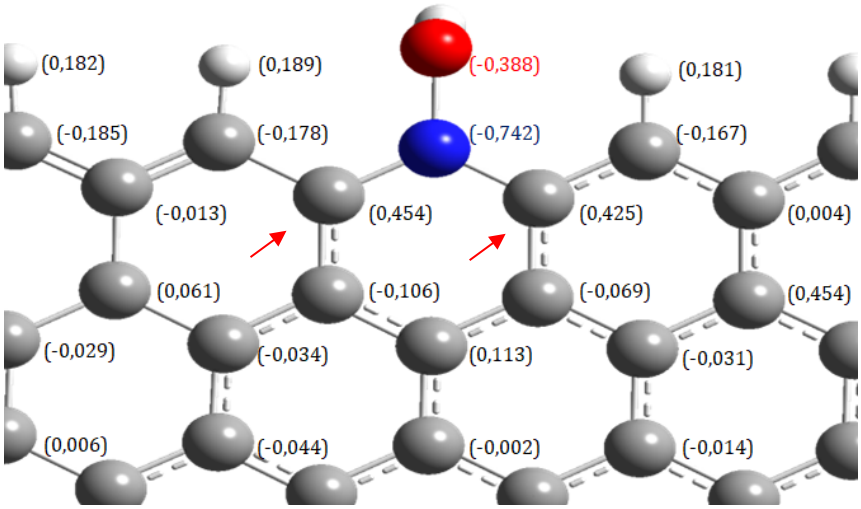

Figure S10. Model structures and atom effective charge of oxidized nitrogen in zigzag position where the blue spheres correspond to nitrogen atom, red spheres correspond to oxygen atom, grey spheres correspond to carbon atom and white spheres correspond to hydrogen atom.

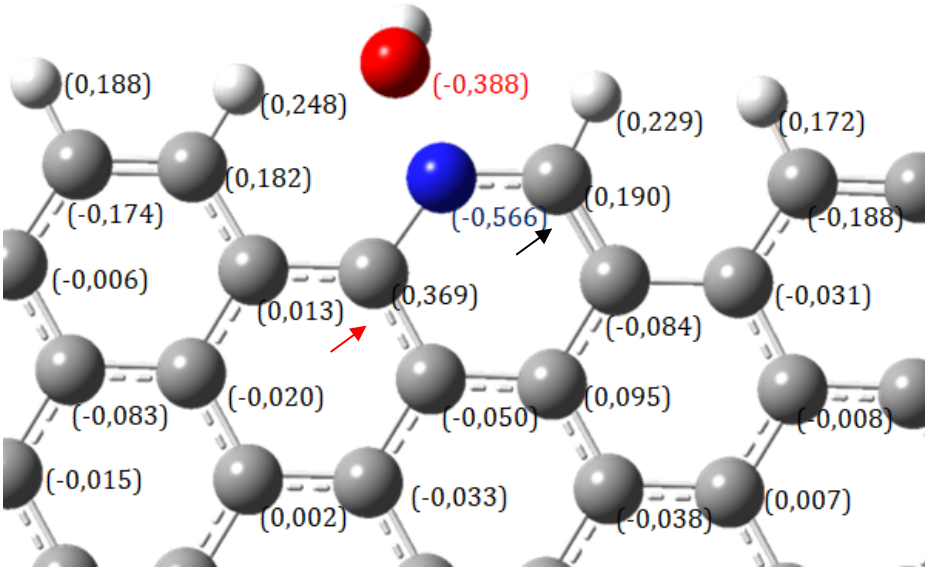

Figure S11. Model structures and atom effective charge of oxidized nitrogen in armchair position where the blue spheres correspond to nitrogen atom, red spheres correspond to oxygen atom, grey spheres correspond to carbon atom and white spheres correspond to hydrogen atom.

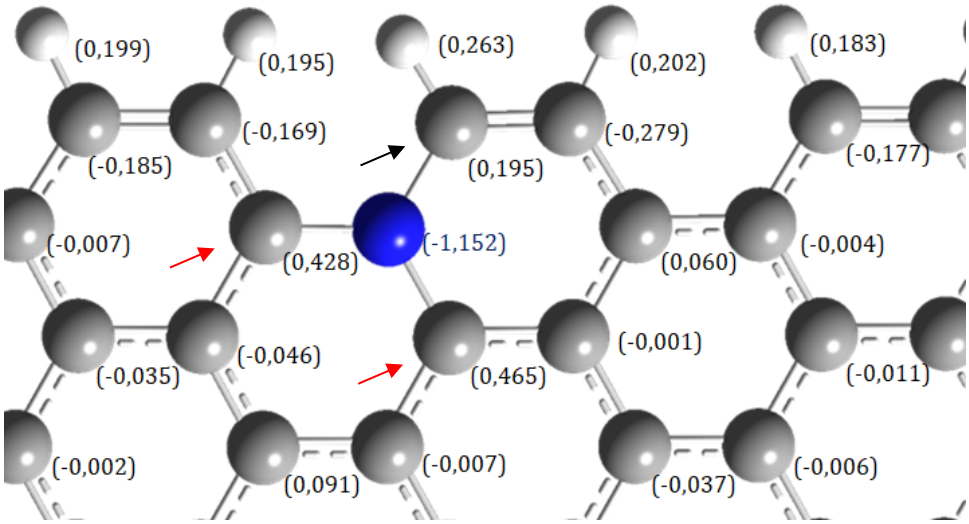

Figure S12. Model structures and atom effective charge of quaternary nitrogen in armchair position where the blue spheres correspond to nitrogen atom, grey spheres correspond to carbon atom and white spheres correspond to hydrogen atom.

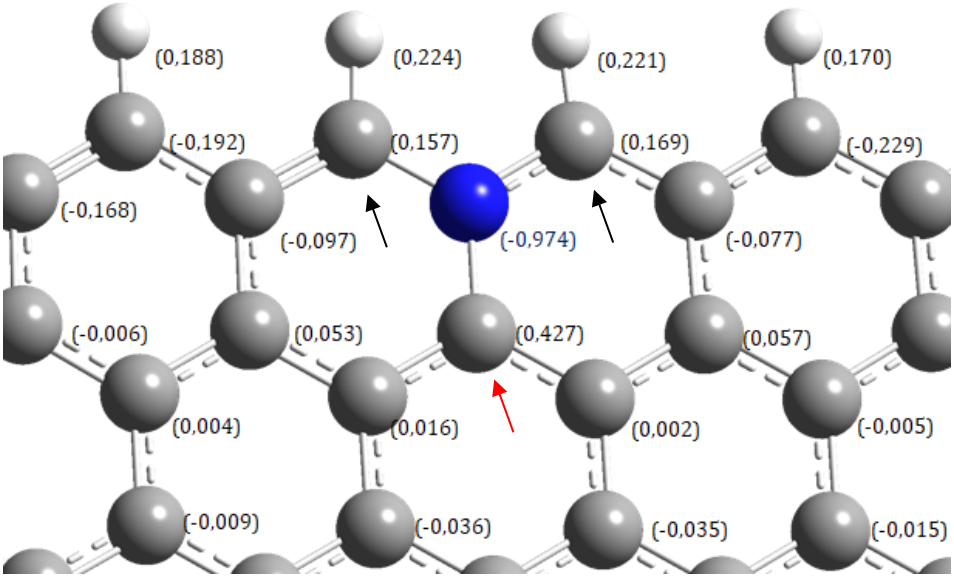

Figure S13 Model structures and atom effective charge of quaternary nitrogen in zigzag position where the blue spheres correspond to nitrogen atom, grey spheres correspond to carbon atom and white spheres correspond to hydrogen atom.

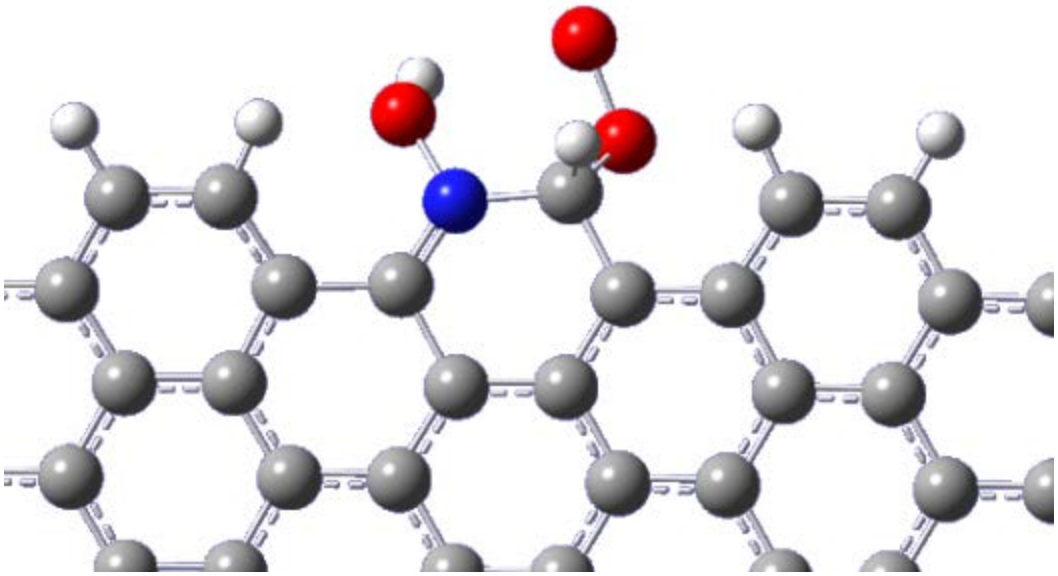

Figure S14: Model structure of the oxygen reduction reaction intermediate product in N-O species in armchair position.

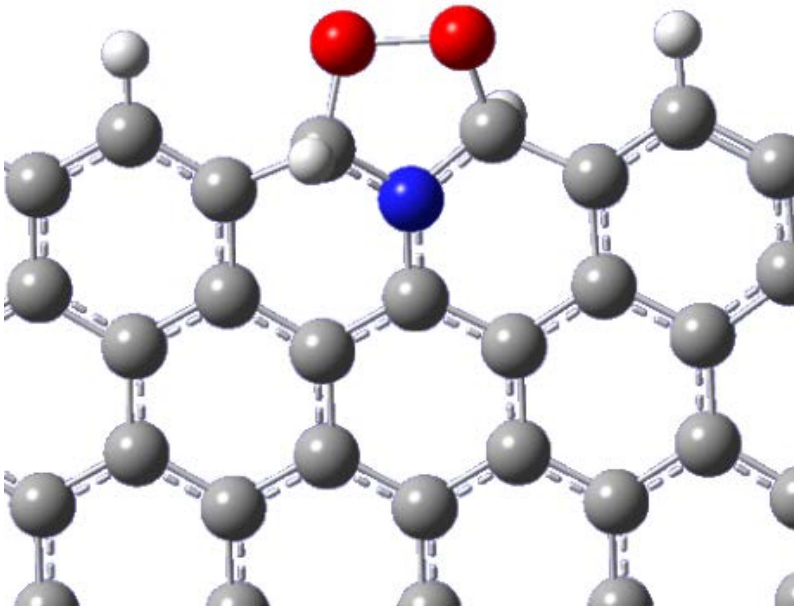

Figure S15: Model structure of the oxygen reduction reaction intermediate product in quaternary N species in zigzag position.

Table S2: Comparison on the electrocatalytic activity of the recently reported ORR catalysts.

Catalyst	*Mass used / mg cm^{-2}*	*Onset potential / V*	*Half-wave potential / V*	*Limiting current / -mA cm^{-2}*	*Number of electrons*	*Reference*
PANI_1100	**0.48**	**0.94**	**0.85**	**5.4**	**3.9 (RRDE)/ 4.0 (KL)**	**This work**
20wt% Pt/Vulcan	0.41	0.98	0.84	5.4	4.0 (RRDE) / 4.0 (KL)	This work
PANId_O2_800	0.48	0.75	0.66	5.2	3.0 (RRDE)	S3
NA-NCNT/GC	-	0.95	-	Not showed and not achieved	3.9 (RRDE)	S4
N-RG-O 1000ºC	0.5	0.85	0.66	4.2	2.25 (KL)	S5
N-graphene	-	0.82	0.68	0.8 (at 1000rpm)	3.6 (KL)	S6
PDMC800	0.1	0.85	-	Not achieved	3.2 (KL)	S7
N 550-GD	0.4	0.84	0.68	4	3.7 (KL)/ 3.7 (RRDE)	S8
PDI-900/GC	0.1	0.82	0.75	Not achieved	3.9 (KL)	S9
g-C3N4@CMK-3	0.084	0.88	-	Not achieved	4 (KL)	S10
N-CN	0.2	0.80	0.70	4	3.5 (KL)	S11
N-HCNSs	0.4	0.85	0.75	3.0	-	S12

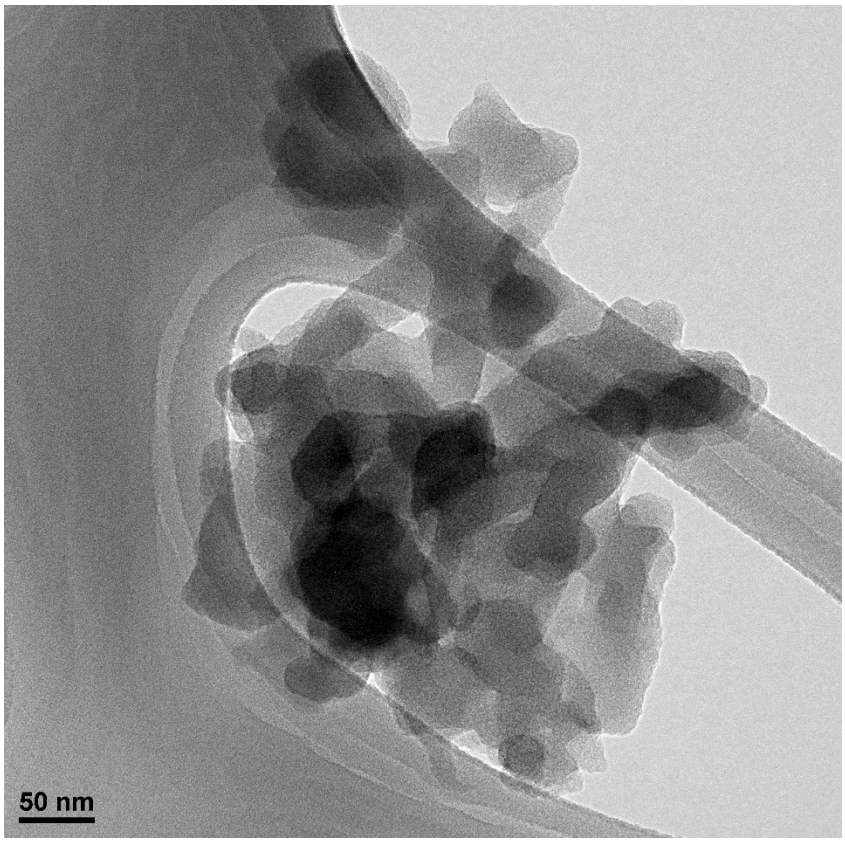

Figure S16: TEM image of PANI_1100 at low magnification.

Notes and references

S1. H. Marsh and F. Rodríguez-Reinoso, *Activated Carbon*, 1st Edition, Elsevier, 2006, ISBN: 9780080455969, Chapter 2, page. 30.

S2. F. XU, D. Wu, R. Fu and D. Wei, *Materials Today*, 2017, **20**, 629.

S3 J. Quílez-Bermejo, C. González-Gaitán, E. Morallón and D. Cazorla-Amorós, *Carbon*, 2017, **119**, 62-74

S4 K. Gong, F. Du, Z. Xia, M. Durstock and K. Dai, *Science* 2009, **323**, 760.

S5 L. Lai, J. R. Potts, D. Zhan, L. Wang, C. K. Poh, C. Tang, H. Gong, Z. Shen, J. Lin and R. S. Ruoff, *Energy Environ. Sci.*, 2012, **5**, 7936.

S6 Z.J. Lu, S.J. Bao, Y.T. Gou, C.J. Cai, C.C. Ji, M.W. Xu, J. Song and R. Wang, *RSC Adv.*, 2013, **3**, 3990.

S7 R. Silva, D. Voiry, M. Chhowalla and T. Asefa, *J. Am. Chem. Soc.*, 2013, **135**, 7823.

S8 R. Liu, H. Liu, Y. Li, Y. Yi, X. Shang, S. Zhang, X. Yu, S. Zhang, H. Cao and G. Zhang, *Nanoscale*, 2014, **6**, 11336.

S9 R. Liu, D. Wu, X. Feng and K. Müllen, *Angew. Chemie - Int. Ed.*, 2010, **49**, 2565.

S10 Y. Zheng, Y. Jiao, J. Chen, J. Liu, J. Liang, A. Du, W. Zhang, Z. Zhu, S. C. Smith, M. Jaroniec, G. Q. Max Lu and S. Z. Qiao, *J. Am. Chem. Soc.*, 2011, **133**, 20116

S11 K. Qu, Y. Zheng, S. Dai and S. Z. Qiao, *Nano Energy*, 2016, **19**, 373.

S12 T. Yang, J. Liu, R. Zhou, Z. Chen, H. Xu, S. Z. Qiao and M. J. Monteiro, *J. Mater. Chem. A*, 2014, **2**, 18139.